Research Article

Finite-Difference Time-Domain Solution of a Memristor Fed by a Transmission Line

Tuğba Nur Batmaz[1]* **and Reşat Mutlu[2]**

Namık Kemal University, Department of Electronic and Communication Engineering, Corlu, Tekirdag, Turkey[1]
Çorlu Mühendislik Fakültesi, Tekirdağ Namık Kemal Üniversitesi, Tekirdağ, Türkiye[2]

Abstract- Memristor is a new nonlinear circuit element. Examination of its use with other circuit elements is important from Circuit analysis point of view. A memristor connected at the end of a transmission line will exhibit a different behavior than a resistor does. It is difficult or impossible to solve such a problem since the memristor is a nonlinear circuit element. In this study, the equation of the electromagnetic wave propagating over the transmission line with a memristor load is solved using the finite-difference time-domain (FDTM) method. Memristor current and voltage are calculated depending on time. The simulations are made with the MATLAB program.

Keywords: FDTD, Memristor, Transmission Line, Reflection analysis.

Bir İletim Hattından Beslenen Bir Memristörün Zamanda Sonlu Farklar Yöntemi İle Çözümü

Özet: Memristör yeni bir doğrusal olmayan devre elemanıdır. Diğer devre elemanları ile birlikte kullanımın incelenmesi Devre analizi açısından önemlidir. Bir iletim hattının sonuna bağlanan memristör elemanı bir dirence göre daha farklı bir davranış sergileyecektir. Memristor nonlineer bir devre elemanı olduğu için, böyle bir problemin çözümünün yapılması zor ya da imkansızdır. Bu çalışmada, bir memristor ile yüklü bir iletim hattının üzerinde yayılan elektromanyetik dalganın denklemi Zaman Domeninde Sonlu Farklar (ZDSF) yöntemi kullanılarak çözülmüştür. Memristör akımı ve gerilimi zamana bağlı olarak hesaplanmıştır. Simülasyonlar MATLAB programı ile yapılmıştır.

Anahtar Kelimeler: FDTD, Memristör, İletim hattı, Yansıma analizi

*Corresponding author:
 E-mail address:* tugbanurbatmaz@gmail.com (T. Batmaz)

1. Introduction

The finite-difference time-domain (FDTM) method is widely used in solving electromagnetic problems and wave equations [1-3]. This method was first proposed by Kane Yee to apply finite difference operators centered on graded grids in space and time for an electric and magnetic vector field in Maxwell's equations [4]. Transmission lines are widely used in data communication [11]. Modeling communication cables is a very complex and difficult process. The transmission lines or cables are also commonly examined in literature using numerical methods such FDTD, finite elements, etc. [5-10]. Transmission lines are modeled using the telegrapher equation developed by Heaviside [11-13]. Transmission lines feeding common circuit elements such as resistor, capacitor, and inductor have solutions in the frequency and time domain and are widely used in engineering [11]. Cable electrical parameters such as resistance, inductance, capacitance, leakage conductance per unit length are given in their catalogs and are widely used in their analysis [11, 12-15].

The memristor, whose existence was theoretically predicted in 1971, has become a new nonlinear circuit element [16-21]. The word memristor is created by combining the English words, memory and resistor, and means memory resistor [16]. Therefore, it is a resistor with memory. The electrical resistance of the memristor is called memristance, it depends on the electrical charge which has flown through the device and its value is found as the ratio of its voltage to its current. Analytical solution of an electrical circuit with a memristor is difficult or impossible and approximate or numerical methods are generally used to solve such circuits [22-30]. High frequency applications of the memristor have also been examined in literature [31-33]. If the memristor is fed by a transmission line, this system is a nonlinear system and the FDTD method can be applied to solve this system. According to the literature review, the memristor circuit fed by the transmission line has not been studied yet, but there is a memristor model using finite differences [34]. In this study, a memristor fed by a transmission line has been studied and the numerical solution of the propagating wave equation with FDTD method and the memristor terminal equation is done simultaneously. There are many different memristor models in the literature [35-40]. A memristor may lose Its resistance value when it is fed by a transmission line because of the reflections during transients and that's why it is important to analyze such as circuit. In this study, Biolek's memristor model is used model in all simulations [36]. The system has been simulated in time domain for different source frequencies.

This study is organized as follows. In the second section, transmission line equations are given. In the third section, basic information about a memristor and the Biolek memristor model, which is used in this study, is given. In the fourth section, the FDTD equations necessary for the solution of the system are derived. In the fifth section, the system is simulated. The paper is concluded with the last section.

2. The Lossy Transmission Line Equations

The lossy transmission line equations, also known as Telegrapher's Equations, are based on Maxwell's equations. First order current and voltage equations describing a lossy transmission line are given as

$$\frac{\partial V(z,t)}{\partial z} = -Ri(z,t) - L\frac{\partial i(z,t)}{\partial t} \quad (1)$$

$$\frac{\partial i(z,t)}{\partial z} = -GV(z,t) - C\frac{\partial V(z,t)}{\partial t} \quad (2)$$

where, $V(z,t)$ is the voltage on the line at the position z at time t, $i(z,t)$ is the current flowing through the transmission line at the position z at time t, R is the resistance of the transmission line per unit length (Ohm/m), L is the inductance of the transmission line per unit length (Henry/m), C is the capacitance of the transmission line per unit length (Farad /m), G is the leakage conductance of the transmission line per unit length (Siemens/m).

By doing some algebraic manipulations to Equations 1 and 2, the following second order linear differential equations of a transmission line are obtained for line voltage and line current:

$$\frac{\partial^2 V(z,t)}{\partial z^2} = LC\frac{\partial^2 V(z,t)}{\partial t^2} + RC\frac{\partial V(z,t)}{\partial t} + RGV(z,t) \quad (3)$$

$$\frac{\partial^2 i(z,t)}{\partial z^2} = LC\frac{\partial^2 i(z,t)}{\partial t^2} + RC\frac{\partial i(z,t)}{\partial t} + RGi(z,t) \quad (4)$$

3. Memristor ve Biolek's Memristor Model

A memristor model with nonlinear dopant drift is given as

$$v_{mem}(t) = R_{mem}(x)i_{mem}(t) \quad (5)$$

$$\frac{dx}{dt} = \frac{\mu_v R_{on}}{D^2} i_{mem}(t) f(x,i) \quad (6)$$

where v(t) is the memristor voltage, $i(t)$ is the memristor current, $R(x)$ is the memristor memristance or resistance, x=w/D is the memristor state variable or the normalized doped region length of memristor, w is the doped length of the memristor, D is the total memristor element length, μ_V is the mobility of the memristor element, $f(x,i)$ is the polarity dependent of the window function of the memristor.

The memristor electrical resistance is linearly dependent on the state variable $x(t)$. The state variable $x(t)$ takes the values between 0 and 1. Memristor's memristance and resistance:

$$R_{mem}(x) = R_{off} - \left(R_{off} - R_{on}\right)x \quad (7)$$

where R_{off} and R_{on} are the memristor's maksimum and minimum resistance.

There are lots of different window functions in the literature [35-40]. The window function of the Biolek's memristor model is used in this study and it can be expressed as:

$$f(x,i_{mem}) = 1 - (x - step(-i_{mem})^{2p} \quad (8)$$

where step( ) is the unit step function..

$$f(x,i_{mem}) = \begin{cases} 1-(x-step(-i_{mem})^{2p} & ,i_{mem}<0 \\ 1-x^{2p} & ,i_{mem}\geq0 \end{cases} \quad (9)$$

The window function is dependent of the parameter p. Using a piece-wise linear function, the derivative of the state variable x can also be expressed as

$$\frac{dx}{dt} = \frac{\mu_v R_{on} i_{mem}(t)}{D^2} \begin{cases} 1-(x-step(-i_{mem}(t))^{2p} & ,i_{mem}<0 \\ 1-x^{2p} & ,i_{mem}\geq0 \end{cases} \quad (10)$$

The memristor is simulated for the parameters given in Table 1. The parameters have been chosen considering the parameter data provided in literature and R_{ON} is chosen as greater than R_{ON}, which is a condition that should be satisfied for the ionic memristors [18-19, 21, 23]. The simulated hysteresis loops of the memristor model for 3 different operation frequencies can be seen in Figure 1. The memristor voltage and current for the frequencies are shown in Figure 2. At high freuqeuncies, the area of the hysteresis loop of the memristor gets smaller and memristor starts behaving as an LTI resistor as seen in Figure 2. Also, the memristor gets saturated at 100 kHz as seen in Figure 1. The memristor hysteresis loop is not symmetric due to the current dependency at 100 kHz and 1 MHz as seen in Figure 1. The memristor current at 100 kHz and 1 Mhz frequencies has more harmonics and it does not have half-wave symmetry due to current dependency which results in a DC bias seen in

Figure 2. At 10 MHz, the memristor behaves almost as if a LTI resistor, the DC offset in the current is hard to see, and the current is almost sinusoidal as shown in Figure 3.c.

Table 1 Memristor parameters used in the simulations.

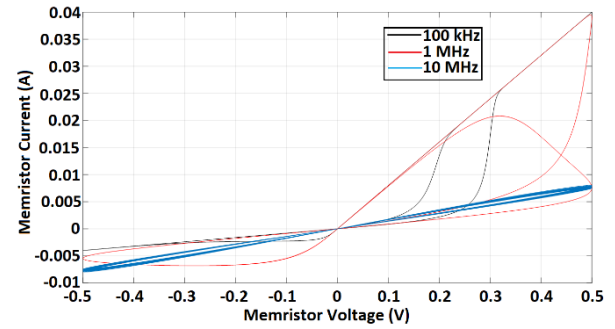| The memristor minimum resistance	R_{ON}	10 Ω
The memristor maximum resistance	R_{OFF}	100 Ω
The dopant mobility	μ	40.10^{-14} m^2/V.s
The memristive element length	D	10 nm
Power parameter in the Biolek's window function	p	2

Figure 1. Hysteresis Curves of memristor model for x(0)=0.5 and 100 kHz, 1 MHz, and 10 MHz.
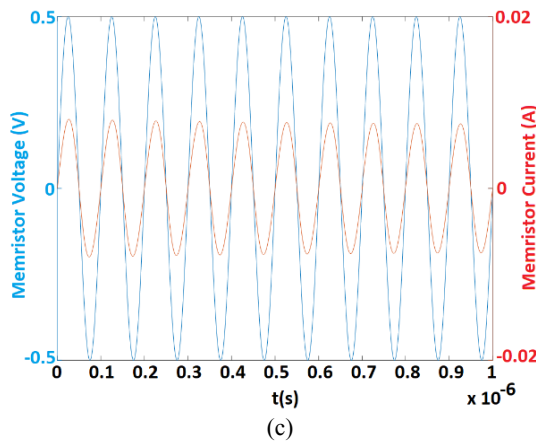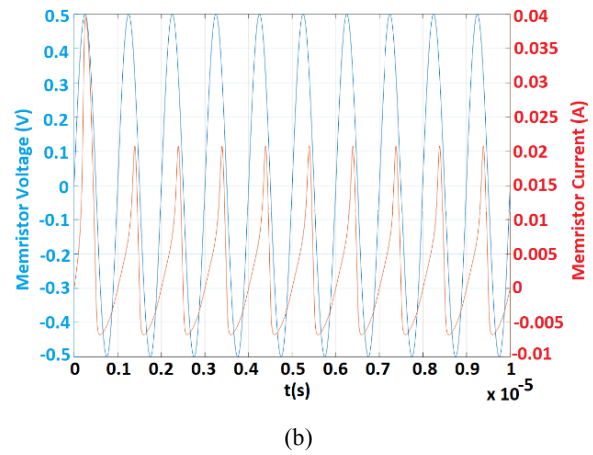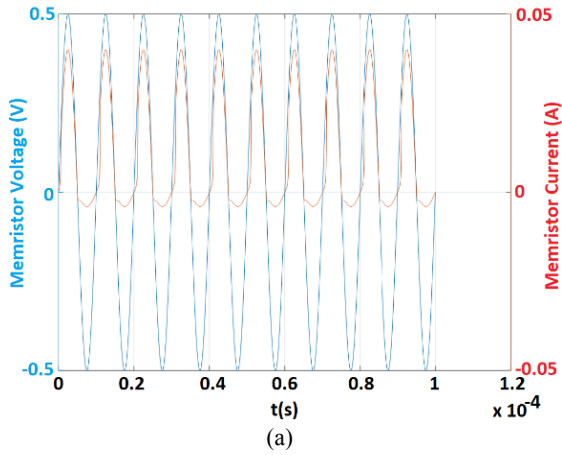

(a)

(b)

(c)

Figure 2. Memristor Voltage (blue) and Memristor Current (red) versus time for x(0)=0.5 and for a) 100 kHz, b) 1 Mhz, and c) f=10 MHz.

4. Derivation of Finite-Difference Time-Domain Equations for a Transmission Line-fed Memristor

Figure 3 shows a memristor fed by a transmission line. In this section, the lossy transmission line equations is solved using the finite difference method. The potential on a transmission line is given as $V(z,t)$. Therefore, it depends on both position and time.
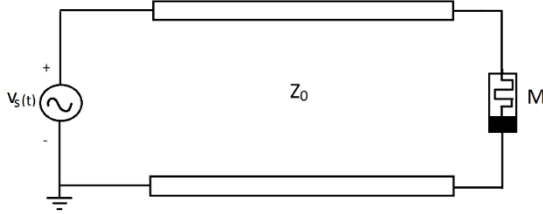

Figure 3. Transmission line-fed memristor system.

Using finite difference method, the difference equations can be obtained:

$$\frac{\partial^2 V(z,t)}{\partial z^2} \approx \frac{V(z+\Delta z,t)-2V(z,t)+V(z-\Delta z,t)}{\Delta z^2} \quad (11)$$

$$\frac{\partial^2 V(z,t)}{\partial t^2} \approx \frac{V(z,t+\Delta t)-2V(z,t)+V(z,t-\Delta t)}{\Delta t^2} \quad (12)$$

$$\frac{\partial V(z,t)}{\partial t} \approx \frac{V(z,t+\Delta t)-V(z,t)}{\Delta t} \quad (13)$$

where Δt is the time step and Δz is the line position increment.

Substituting difference equations into the voltage wave equation given by Eq. (3), $V(z,t+\Delta t)$ is obtained as the follows.

$$V(z,t+\Delta t) = \frac{V(z+\Delta z,t)+V(z-\Delta z,t)}{\Delta z^2\left(\frac{LC}{\Delta t^2}+\frac{RC+LG}{\Delta t}\right)}$$
$$-\frac{LCV(z,t-\Delta t)}{\Delta t^2\left(\frac{LC}{\Delta t^2}+\frac{RC+LG}{\Delta t}\right)} \quad (14)$$
$$-\frac{\left(\frac{2LC}{\Delta t^2}-\frac{2}{\Delta z^2}+\frac{RC+LG}{\Delta t}-RG\right)}{\left(\frac{LC}{\Delta t^2}+\frac{RC+LG}{\Delta t}\right)}V(z,t)$$

While programming instead of t and, the indices k and n are used in the transmission line variables and the following expressions can be written:

$$V(n,k+1) = \frac{V(n+1,k)+V(n-1,k)}{\Delta z^2\left(\frac{LC}{\Delta t^2}+\frac{RC+LG}{\Delta t}\right)}$$
$$-\frac{LCV(n,k-1)}{\Delta t^2\left(\frac{LC}{\Delta t^2}+\frac{RC+LG}{\Delta t}\right)} \quad (15)$$
$$-\frac{\left(\frac{2LC}{\Delta t^2}-\frac{2}{\Delta z^2}+\frac{RC+LG}{\Delta t}-RG\right)}{\left(\frac{LC}{\Delta t^2}+\frac{RC+LG}{\Delta t}\right)}V(n,k)$$

The ranges of the line position z and time t,

$$0 \leq z \leq \ell \quad (16)$$

And

$$0 \leq t \leq T_{end} \quad (17)$$

where ℓ is the line length and T_{end} is the simulation time.

Matlab is used for coding. In Matlab, matrix indexes cannot be negative or zero.

The time step is:

$$\Delta t = \frac{\ell}{N_t} \quad (18)$$

where N_t+1 is the number of the time steps of the simulation.

The position increment is:

$$\Delta z = \frac{\ell}{N_z} \quad (19)$$

where N_z+1 is the number of the line positions of the simulation.

Therefore,

$$1 \leq k \leq N_t+1 \quad (20)$$

And

$$1 \leq n \leq N_z+1 \quad (21)$$

At the end of the line, the memristor is connected as the load and its current is given as:

$$i_{mem}(t) = \frac{v_{mem}(t)}{R_{mem}(x(t))} \quad (22)$$

Using Euler method to solve Biolek's memristor model, the following equations are obtained and they should be computed at each time step.

$$x(t+\Delta t) = \frac{\mu_v R_{on}\Delta t}{D^2}i_{mem}(t)f(x(t),i_{mem}(t))$$
$$+x(t) \quad (23)$$

In programming, the index k is used in the memristor variables and the following expressions can be written:

$$x(k+1) = \frac{\mu_v R_{on}\Delta t}{D^2}i_{mem}(k)f(x(k),i_{mem}(k))$$
$$+x(k) \quad (24)$$

$$R_{mem}(k) = R_{off} - \left(R_{off}-R_{on}\right)x(k) \quad (25)$$

$$i_{mem}(k) = \frac{v_{mem}(k)}{R_{mem}(k)} \quad (26)$$

Eq. 15 and Eqs. 24-26 should be connected together. Using

the FDTD method for Eq. (1), the following difference equations are obtained:

$$\frac{\partial V(z,t)}{\partial z} \approx \frac{V(z+\Delta z,t)-V(z,t)}{\Delta z} \tag{27}$$

And

$$\frac{\partial i(z,t)}{\partial t} \approx \frac{i(z,t+\Delta t)-i(z,t)}{\Delta t} \tag{28}$$

Therefore, Eq. (1) can be approximated as

$$\frac{V(z+\Delta z,t)-V(z,t)}{\Delta z} = -Ri(z,t)$$
$$-L\frac{i(z,t+\Delta t)-i(z,t)}{\Delta t} \tag{29}$$

Using indices n and k, Eq. (29) can be written as

$$\frac{V(n+1,k)-V(n,k)}{\Delta z} = -Ri(n,k)$$
$$-L\frac{i(n,k+1)-i(n,k)}{\Delta t} \tag{30}$$

At the end of the transmission line, the memristor current is equal to the line current:

$$i_{mem}(t) = i(\ell,t) = \frac{v_{mem}(t)}{R_{mem}(x(t))} \tag{31}$$

Using indices n and k, Eq. (31) can be written as

$$i_{mem}(k) = i(N_z+1,k) = \frac{v_{mem}(k)}{R_{mem}(k)} \tag{32}$$

At the end of the transmission line (at $n = N_z + 1$), Eq. (30) turns into

$$\frac{V(N_z+1,k)-V(N_z,k)}{\Delta z} = -Ri(N_z+1,k)$$
$$-L\frac{i(N_z+1,k+1)-i(N_z+1,k)}{\Delta t} \tag{33}$$

Where

$$i(N_z+1,k+1) = i_{mem}(k+1) = \frac{v_{mem}(k+1)}{R_{mem}(k+1)} \tag{34}$$

By solving the Eq.s 15, 24-26, 32-34 simultaneously in Matlab, the memristor voltage can be found numerically using finite difference method.

5. Simulations

The simulations for the transmission line-fed memristor

system are performed in this section. Memristor and transmission line parameters given in Tables 1 and 2 are used in simulations. The waveforms shown in Figures 4-7 are obtained from the simulations. Due to space considerations, simulation results are given for only two frequencies. Memristor voltage, current, and resistance are shown in Figure 4 for f=2 MHz and V_m=0.25 Volt. The source voltage is applied to the line at t=0 and its effect is felt after the wave propagates through the transmission line almost 1 microsecond later. The memristor voltage and current has different amplitudes for each polarity as seen in Figure 4. As shown in Figure 4.c, the memristive switching occurs and the memristor switches to the minimum resistance state and stays at that value due to the high operation frequency in steady-state. The voltage and current of the transmission line depend not only on the position but also on time. Also, the voltage distribution on the transmission line is illustrated for several different times in Figure 5. The voltage wave does not arrive at the memristor load not until one microsecond passes as seen in Figures 5.a and 5.b. The voltage wave turns into a standing wave after the memristor completes its resistive switching in the steady-state as shown in Figure 5.f. The wavelength of the voltage wave can be seen in Figure 5. The wave nature and attenuation of the line voltage are also apparent in Figure 5.

Table 2 Transmission line parameters used in the simulations.

The cable resistance per unit length	R	0.001 Ω/m
The cable capacitance per unit length	C	100 pF/m
The cable inductance per unit length	L	25.10^{-8} H/m
The cable leakage conductance per unit length	G	10 (mΩ/m)
Cable length	ℓ	200 m

If the frequency decreases to 200 kHz, the memristor voltage is shown in Figure 6. The memristor goes through a transient state and, after multiple reflections, the output or the memristor voltage reaches the steady-state as shown in Figure 6. An exponential-like transient can be seen in Figure 6. The electromagnetic wavelength is higher than the line length of 200 meter at 200 kHz and the voltage distribution on the line at t=2.5 Microseconds is given in Figure 7 in this case. At such a low frequency, instead of solving the transmission line equations, the transmission line can be modeled as a resistor-inductor series circuit. The simulations show that the circuit programs must take memristor loads into account and FD method can easily allow examining transmission feeding a memristor load.
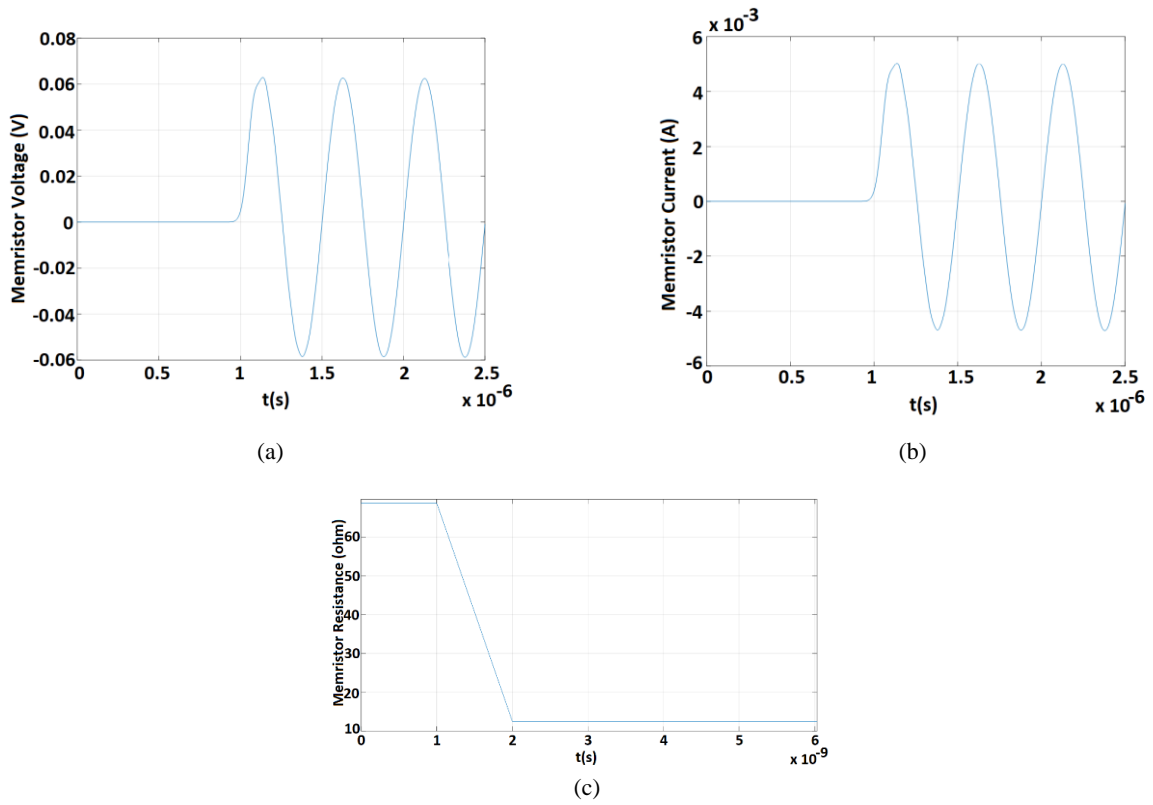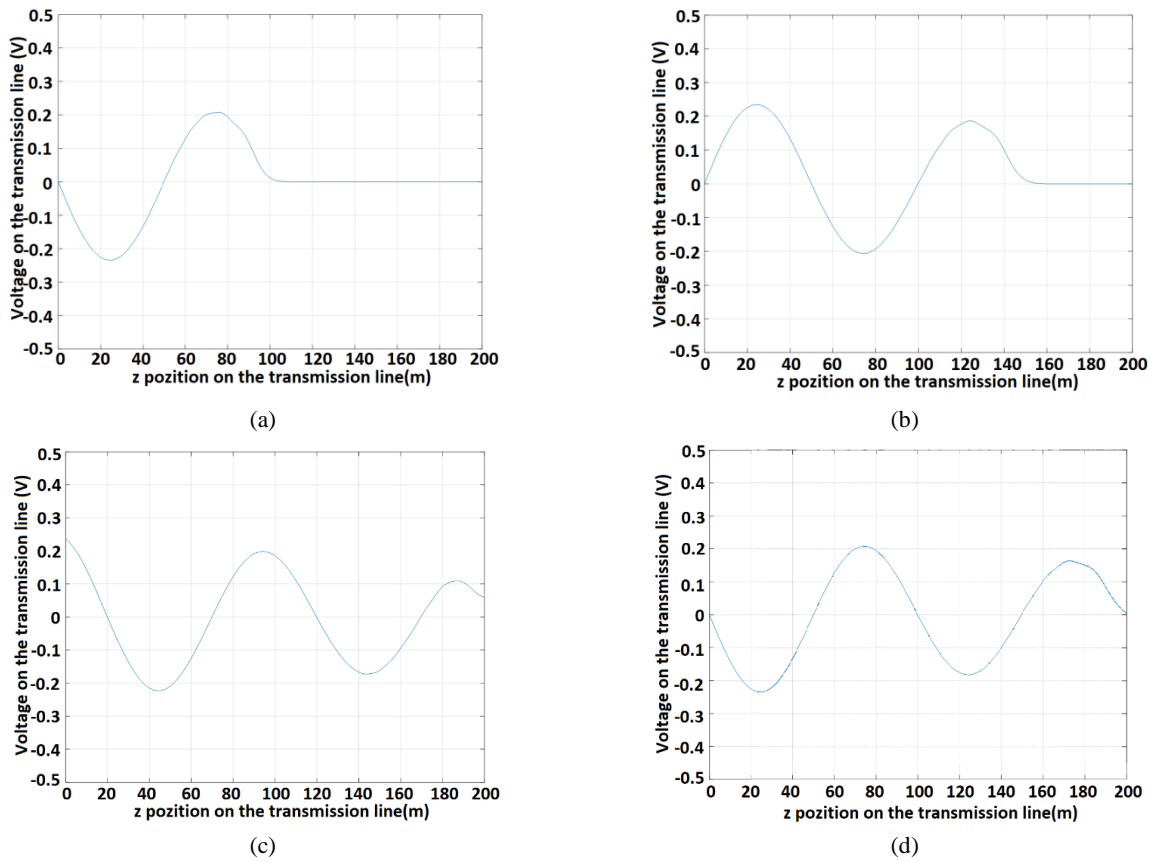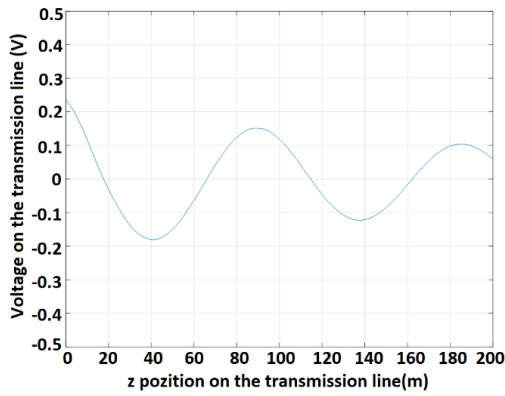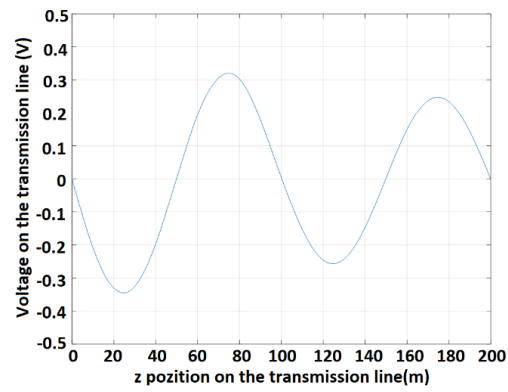
(a)

(b)

(c)

Figure 4. a) Memristor Voltage, b) Memristor Current, and c) Memristor Resistance for f=2 MHz and V_m=0.25 Volt.

(a)

(b)

(c)

(d)

(e)

(f)

Figure 5. Voltage distribution on the transmission line for f=2 MHz and V_m=0.25 Volt at a) t=0.5 Microseconds, b) t=0.75, c) t=1.1, d) t=1.5, e) t=2.1, and f) t= 2.5 Microseconds.
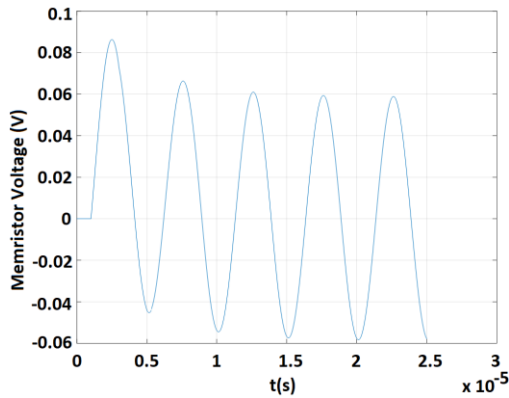

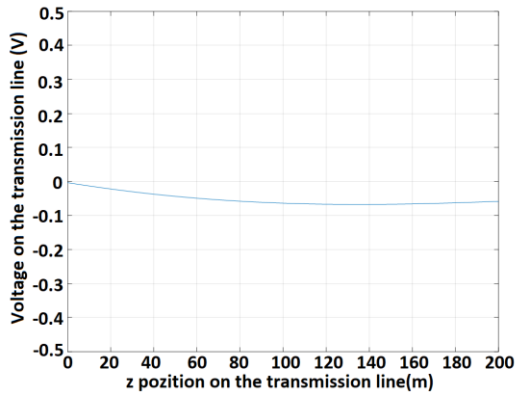**Figure 6.** Memristor Voltage for f=200 kHz and V_m=0.25 Volt

Figure 7. Voltage distribution on the transmission line for f=200 kHz and V_m=0.25 Volt at t=2.5 Microseconds.

6. Conclusions

In this study, transmission line equations are solved for a memristor load. The memristor powered by the transmission line has been simulated for two different frequencies. It has been observed that with increasing frequency, the memristor acts as a linear resistor as expected. After multiple reflections, the output voltage reaches the steady-state. While the reflections from both ends of the line continues, the memristance of the memristor varies somewhat. In the transient regime, the memristance of the memristor can change or deviate from its initial value. The change is higher at low frequencies. A full memristive switching can occur at very low frequencies. The change may also not negligible at higher frequencies due to nonlinearity of the window function of memristor. As a result, precautions should be taken when the memristor is connected to the end of a transmission line in high frequency circuits. The effect of the reflections from both ends of the transmission line during the transient regime must be considered in designing such a circuit perhaps using a FDTD solution method as done in this study. We suggest frequency domain analysis of such a circuit as future study.

References

[1] Taflove, A., & Hagness, S. C. (2005). Computational electrodynamics: the finite-difference time-domain method. Artech house.

[2] Shlager, K. L., & Schneider, J. B. (1995). A selective survey of the finite-difference time-domain literature. IEEE Antennas and Propagation Magazine, 37(4), 39-57.

[3] Sadiku, M. N. (2018). Numerical techniques in electromagnetics with MATLAB. CRC press.

[4] Yee, K. (1966). Numerical solution of initial boundary value problems involving Maxwell's equations in isotropic media. IEEE Transactions on antennas and propagation, 14(3), 302-307.

[5] Komisarek, K. S., Chamerberlin, K. A., & Sivaprasad, K. (1993). A method of moment analysis of a twisted-pair transmission line. In Proceedings of IEEE Antennas and Propagation Society International Symposium 1993 (pp. 64-67). IEEE.

[6] Roden, J. A., Gedney, S. D., & Paul, C. R. (1996). A rigorous analysis of twisted pair transmission lines using non-orthogonal FDTD and the PML absorbing boundary condition. In Proceedings of Symposium on Electromagnetic Compatibility (pp. 254-258). IEEE.

[7] Poltz, J., Gleich, D., Josefsson, M., & Lindstrom, M. (2000). Electromagnetic modeling of twisted pair cables. In Proceedings of the 49th International Wire and Cable symposium. International Wire and Cable Symposium, 2000.

[8] Kirawanich, P., Islam, N. E., & Yakura, S. J. (2006). An electromagnetic topology approach: Crosstalk

characterizations of the unshielded twisted-pair cable. Progress In Electromagnetics Research, 58, 285-299.

[9] Liu, X. (2006). Low pressure partial discharge investigation with FEM modeling for a twisted pair of insulated conductors. In 2006 IEEE Conference on Electrical Insulation and Dielectric Phenomena (pp. 611-614). IEEE.

[10] Tatematsu, A., Rachidi, F., & Rubinstein, M. (2016). A technique for calculating voltages induced on twisted-wire pairs using the FDTD method. IEEE Transactions on Electromagnetic Compatibility, 59(1), 301-304.

[11] Pozar, D. M. (1998). Microwave engineering, John Wiley & Sons. Inc.

[12] Heaviside, O. (1876). XIX. On the extra current. The London, Edinburgh, and Dublin Philosophical Magazine and Journal of Science, 2(9), 135-145.

[13] Miano, G., & Maffucci, A. (2001). Transmission lines and lumped circuits: fundamentals and applications. Elsevier.

[14] Reçber Kablo Datasheet (2021, 19 December), retrieved from, https://www.recber.com.tr/pdf/urun-katalog.pdf

[15] Öztürk, P., ALİSOY, H., & Mutlu, R. (2019)Yapay Sinir Ağları Kullanarak İkili ve Üçlü Büküm Makinaların Ürettiği CAT 6A U/FTP Kabloların Parametrelerinin Tahmini ve Tahmin Edilen Sonuçların Karşılaştırılması. European Journal of Engineering and Applied Sciences, 2(2), 41-51.

[16] Chua, L. (1971). Memristor-the missing circuit element. IEEE Transactions on circuit theory, 18(5), 507-519.

[17] Chua, L. O., & Kang, S. M. (1976). Memristive devices and systems. Proceedings of the IEEE, 64(2), 209-223.

[18] Strukov, D. B., Snider, G. S., Stewart, D. R., & Williams, R. S. (2008). The missing memristor found. nature, 453(7191), 80-83.

[19] Williams, R. S. (2008). How We Found The Missing Memristor IEEE Spectrum, 45(12), 28-35.

[20] Kavehei, O., Iqbal, A., Kim, Y. S., Eshraghian, K., Al- Sarawi, S. F., & Abbott, D. (2010). The fourth element: characteristics, modelling and electromagnetic theory of the memristor. Proceedings of the Royal Society A: Mathematical, Physical and Engineering Sciences, 466(2120), 2175-2202.

[21] Mazumder, P., Kang, S. M., & Waser, R. (2012). Memristors: devices, models, and applications. Proceedings of the IEEE, 100(6), 1911-1919.

[22] Wang, F. Y. (2008). Memristor for introductory physics. arXiv preprint arXiv:0808.0286.

[23] Joglekar, Y. N., & Wolf, S. J. (2009). The elusive memristor: properties of basic electrical circuits. European Journal of physics, 30(4), 661.

[24] Mutlu, R. (2015). Solution of TiO_2 memristor-capacitor series circuit excited by a constant voltage source and its application to calculate operation frequency of a programmable TiO_2 memristor-capacitor relaxation oscillator. Turkish Journal of Electrical Engineering & Computer Sciences, 23(5), 1219-1229.

[25] Bayır Ö., & Mutlu R. (2013). Investigation of Memristor-Inductor Series Circuit under DC Excitation Using a Piecewise Memristor Characteristic, 6. İleri Muhendislik Teknolojileri Sempozyumu 2013. Çankaya Üniversitesi

[26] Yener, S. C., Mutlu, R., & Kuntman, H. H. (2015). A new memristor-based low-pass filter topology and its small- signal solution using MacLaurin series. SAT, 1(1), 2.

[27]Yener, S. C., Mutlu, R., & Kuntman, H. H. (2018). Small signal analysis of memristor-based low-pass and high-pass filters using the perturbation theory. Optoelectronics and Advanced Materials-Rapid Communications, 12(January-February 2018), 55-62.

[28] Mutlu, R. (2018). AC Power Formula for Unsaturated TiO2 Memristors with Linear Dopant Drift, Small Signal AC Power Formula for All Memristors, and Some Applications for These Formulas. European Journal of Engineering and Applied Sciences, 1(2), 1-8.

[29] Mutlu R. (2010). Taylor Serisi ve Kutupsal Fonksiyonlar Kullanarak Memristorün (Hafızalı Direncin) Histeresis Eğrisinin Açıklanması. 3. Ileri Muhendislik Teknolojileri Sempozyumu 2010 (pp. 401–408). Çankaya University.

[30] Urgan, N. N., Dalmış, C., & Mutlu, R. (2021). Analysis of the HP Memristor and Capacitor (MC) Series Circuit Using the Lambert W Function. European Journal of Engineering and Applied Sciences, 3(2), 27-32.

[31] Kvatinsky, S., Friedman, E. G., Kolodny, A., & Weiser, U. C. (2013). The desired memristor for circuit designers. IEEE Circuits and Systems Magazine, 13(2), 17-22.

[32] Potrebić, M., Tošić, D., & Biolek, D. (2017). Rf/microwave applications of memristors. In Advances in Memristors, Memristive Devices and Systems (pp. 159-185). Springer, Cham.

[33] Potrebic, M., & Tosic, D. (2015). Application of memristors in microwave passive circuits. Radioengineering, 24(2), 408-419.

[34] Yang, Z., & Tan, E. L. (2015). Two finite-difference time-domain methods incorporated with memristor. Progress In Electromagnetics Research, 42, 153-158.

[35] Yang, J. J., Pickett, M. D., Li, X., Ohlberg, D. A., Stewart, D. R., & Williams, R. S. (2008). Memristive switching mechanism for metal/oxide/metal nanodevices. Nature nanotechnology, 3(7), 429-433.

[36] Biolek, Z., Biolek, D., & Biolkova, V. (2009). SPICE Model of Memristor with Nonlinear Dopant Drift. Radioengineering, 18(2), 210-214.

[37] Prodromakis, T., Peh, B. P., Papavassiliou, C., & Toumazou, C. (2011). A versatile memristor model with nonlinear dopant kinetics. IEEE transactions on electron devices, 58(9), 3099-3105.

[38] Zha, J., Huang, H., & Liu, Y. (2015). A novel window function for memristor model with application in programming analog circuits. IEEE Transactions on Circuits and Systems II: Express Briefs, 63(5), 423-427.

[39] Oğuz, Y., Gül, F., & Eroğlu, H. (2017). A New Window Function for Memristor Modeling. In 8th International Advanced Technologies Symposium (IATS17). (pp. 3498- 3502). Elazığ.

[40] Karakulak, E., & Mutlu, R. (2020). SPICE Model of Current Polarity-Dependent Piecewise Linear Window Function for Memristors. Gazi University Journal of Science, 33(4), 776-777.